Pre-mixed precursors for modulating the porosity of carbons for enhanced hydrogen storage: Towards predicting the activation behaviour of carbonaceous matter

Norah Balahmar, and Robert Mokaya*

University of Nottingham, University Park, Nottingham NG7 2RD, U. K.

E-mail: r.mokaya@nottingham.ac.uk (R. Mokaya)

Abstract

Highly porous carbons prepared from pre-mixtures of polypyrrole and raw sawdust or sawdust hydrochar achieve much higher surface area than is possible from single use of any one of the precursors. The pre-mixed precursors offer carbons with ultrahigh surface area (up to 3815 $m^2 g^{-1}$) and pore volume (up to ~2.6 $cm^3 g^{-1}$) comprising of two pore systems in the micropore (6 - 12 Å) and mesopore (22 – 28 Å) range. The porosity can be tailored via choice of pre-mix precursor ratios such that it is possible, under identical activation conditions, to generate carbons that are either microporous or mesoporous. The elemental composition of the precursors and in particular the molar ratio of oxygen to carbon (i.e., O/C molar ratio) is a key variable in determining the development of mesopores, with a high ratio favouring greater mesoporosity. The resulting activated carbons are homogeneous regardless of the pre-mix precursor ratios, and exhibit excellent hydrogen storage capacity that is much higher than can be attained by single-precursor derived samples. The carbons have excess hydrogen uptake (at -196 ºC) of up to 3.6 wt% (at 1 bar) and 6.7 wt% (at 20 bar). The total hydrogen uptake is up to 8.1 wt% (at 20 bar), and 10 wt% (at 40 bar), which is much higher than for most currently available benchmark porous materials. Due to their lower mesoporosity, the pre-mix samples have improved packing density, which means that their volumetric hydrogen uptake (at 40 bar) is much greater (ca. 40 g l^{-1}) than that of single precursor samples (ca. 28 g l^{-1}). The carbons are comparable to or outperform many benchmark materials such as MOFs in terms of their hydrogen uptake, including gravimetric uptake, volumetric uptake and deliverable hydrogen capacity (100 to 5 bar at 77 K). The carbons also have attractive room temperature hydrogen storage capacity. Our findings provide a new method for modulating the porosity of carbons that goes beyond current practice. Furthermore, the new insights on the effect of O/C ratio make it possible to predict the activation behaviour of precursors in a manner that allows optimising porosity of carbons to match specific applications as demonstrated here for hydrogen storage.

1. Introduction

A possible solution to limiting CO_2 emissions to the atmosphere is the use of hydrogen as an energy carrier and/or the capture and storage of CO_2.[1-5] The use of hydrogen for energy production and the capture and sequestration of CO_2 requires materials that can efficiently store and transport gases.[1-7] In the case of hydrogen storage, a wide range of materials have been explored, including porous carbons,[8-18] metal organic frameworks (MOFs),[19-24] and covalent organic frameworks (COFs).[25,26] Carbon-based materials are increasingly receiving attention as energy storage materials in applications that are dependent on their porosity, including storage of energy related gases, and as electrode materials for supercpacitors.[8-18,27-31] This is because carbons, especially activated carbons, offer several attractive features such as controllable porosity, low cost, ready availability, stability (chemical and mechanical), and ease of preparation and handling. The unique structural features of activated carbons are dependent on the nature and type of carbonaceous precursor used, activation method and activation conditions. Activated carbons may be synthesised from a wide range of carbonaceous matter.[18-18,27-36] However, biomass-derived activated carbons are arguably the most attractive due to their being environment-friendly, cheap, readily available, and renewable.[37-42] On the other hand, activated carbons may also be prepared from polymers such polypyrrole or polythiophene, which offer the possibility of conductivity, high levels of mesoporosity and heteroatom doping.[29,33,34,43,44]

To-date, the porosity and other properties of chemically activated carbons are controlled by varying factors such as type of precursor (starting material) and activation conditions (time, temperature and amount of activating agent). Although a wide range of carbonaceous materials are usable as precursors to porous carbons, as far as we are aware, there have been no attempts at the use of pre-mixed precursors as the *only avenue* to controlling, tailoring and/or enhancing the porosity of activated carbons. Furthermore, there

is currently no way to predict the activation behaviour of carbonaceous matter. Recent studies have hinted that the nature of a carbonaceous precursor may have some influence on susceptibility to activation.[13,42,45,46] This is important because the susceptibility to activation is what determines the level and mix of porosity (i.e., proportion and size of micropores and mesopores) generated in the activated carbon. For example, whilst certain biomass-derived carbonaceous matter is relatively resistant to activation and generally yields carbons with significant microporosity,[46] polypyrrole on the other hand is readily activateable and offers carbons that are highly mesoporous.[33] This report, explores the preparation of activated carbons from pre-mixed precursors that contain a mix of carbonaceous materials that are known to respond differently to similar levels of activation. The motivation for the work is three-fold; (i) valorisation of cheap carbonaceous matter to carbons with porosity that is not achievable directly via use of single precursors, (ii) attempts to identify the factors that may allow prediction of the activation behaviour of carbonaceous matter, and (iii) optimisation of the porosity of carbons targeted at high performance hydrogen storage. We, accordingly, report on the use of carbonaceous precursors that contain a polymer (polypyrrole) and eucalyptus wood sawdust *via* either (i) direct activation o*f mixtures* of polypyrrole and raw sawdust, or (ii) conversion of sawdust to hydrochar followed by activation of sawdust hydrochar/polypyrrole mixtures. The activation conditions (i.e., amount of activating agent, activation time and temperature) were kept constant with the ratio of polypyrrole to sawdust or sawdust hydrochar as the only variable for control of porosity. This set-up enabled us to target porosity suitable for hydrogen uptake in a manner that is not achievable via activation of any one of the precursors on their own. Furthermore, the experimental set-up provided new insights on the critical role of the O/C ratio of the carbonaceous precursors in determining the activation behaviour and the extent to which micropores and/or mesopores are generated.

2. Experimental Section

2.1 Material Synthesis

Sawdust from eucalyptus wood was washed with distilled water to remove any impurities, dried in an oven at 120 ^{o}C overnight and sieved to obtain a homogenous particle size ($\leq$ 212 μm) sample designated as SD. Some of the sawdust was converted to hydrochar via hydrothermal carbonization as previously reported.[9,42,47] An aqueous dispersion of the sawdust at a concentration of 320 gL^{-1} (6.4 g of sawdust in 20 ml of water) was placed in a stainless steel autoclave and heated, at a ramp rate of 5 ^{o}C min^{-1}, to 250 ^{o}C for 2 h. The resulting carbon enriched hydrochar, designated as H, was washed with distilled water and dried in an oven at 120 ^{o}C.

Polypyrrole (designated as PPY) was prepared by adding 3 g of pyrrole to 200 mL of 0.5 M $FeCl_3$ solution and stirring the mixture for 2 h at room temperature, as shown in Scheme 1 (Supporting Information). The polypyrrole was recovered, washed with distilled water and dried in an oven at 120 ^{o}C. The yield from pyrrole to polypyrrole was close to 100%.

For activation, two sets of samples were prepared from PPY/SD or PPY/H mixtures. Mixtures of PPY:SD:KOH or PPY:H:KOH at weight ratio of 1:3:4, 1:2:4, 1:1:4 or 2:1:4 were activated at 800 ^{o}C. The amount of KOH and activation temperature were identical for all preparations. The mixtures were ground until homogeneous and placed in a tube furnace and heated under nitrogen for 1 h at the target temperature following a heating ramp rate of 3^{o}C min^{-1}. After cooling, the activated carbons were thoroughly washed with 10 wt% HCl, followed by washing with distilled water until neutral pH was achieved for the filtrate. The activated carbons were dried overnight in an oven at 120 ^{o}C and designated as PPYSD*xyzt* or PPYH*xyzt* where *xyz* is ratio (x:y:z) of the *x* = PPY, *y* = raw sawdust (SD) or hydrochar (H), *z* = KOH, and *t* is temperature of activation (800 °C).

2.2 Materials Characterisation

Elemental (CHN) analysis was performed using an Exeter Analytical CE-440 Elemental Analyser. Thermogravimetric analysis (TGA) curves were obtained on a TA Instruments SDT Q600 analyser under flowing (100 mL/min) air conditions. The porosity of the carbons was determined via nitrogen sorption using a Micromeritics 3FLEX sorptometer. Prior to analysis (at -196 ^{o}C), the carbons were degassed under vacuum at 200 ^{o}C for 12 h. The surface area was calculated using the Brunauer-Emmett-Teller (BET) method applied to adsorption data in the relative pressure (P/P_o) range of 0.04 – 0.22. The total pore volume was determined from the nitrogen uptake at close to saturation pressure ($P/P_o \approx 0.99$). The micropore surface area and micropore volume were determined via *t*-plot analysis. Non-local density functional theory (NL-DFT) applied to nitrogen adsorption isotherms was used to determine the pore size distribution. SEM images were recorded using an FEI Quanta200 microscope, operating at a 5 kV accelerating voltage. Transmission electron microscopy (TEM) images were obtained using a JEOL 2100F instrument operating at 200 kV equipped with a Gatan Orius CCD for imaging. The samples were suspended in distilled water and dispersed onto lacey carbon support film prior to analysis.

2.3 Hydrogen uptake measurements

Hydrogen uptake capacity of the carbons was measured by gravimetric analysis with a Hiden XEMIS Intelligent Gravimetric Analyser using 99.9999% purity hydrogen additionally purified by a molecular sieve filter. Prior to analysis, the carbon samples were dried for 24 h at 80 ^{o}C and then placed in the analysis chamber and degassed at 200 ^{o}C and 10^{-10} bar for 4 – 6 h. The hydrogen uptake measurements were performed at -196 ^{o}C (in a liquid nitrogen bath) over the pressure range of 0 to 100 bar.

3. Results and Discussion

3.1 Properties of Activated Carbons

Given the 'mixed' nature of the starting carbonaceous materials, it was essential to monitor the activation process to ensure that the final activated carbons were homogeneous (one-phase) materials. The surface structure and morphology of the carbon precursors was probed using scanning electron microscopy (SEM), and the images are shown in supporting Figure S1. The morphology of polypyrrole (PPY) consists of globular and spherical particles loosely aggregated into larger assemblies, while the raw sawdust (SD) and sawdust hydrochar (H) show well-defined fibre-like particles with honeycomb holes/voids, typical of lignocellulosic biomass materials or char particles derived from lignocellulosic biomass.[47-49] The morphology of hydrochar, when compared to raw sawdust, shows the effect of hydrothermal treatment; the hydrochar particles appear uneven and with rougher surface topology, which may be ascribed to decomposition of hemicellulose as well as the depolymerisation of cellulose and partial degradation of lignin.[50-53] On activation, however, the resulting activated carbons, regardless of composition of the pre-mixed precursor, show a fairly similar particle morphology (Supporting Figure S2) that is vastly different from that of any of the three precursors (Figure S1). The activated carbons consist of particles with smooth surfaces and large conchoidal cavities. Such a particle morphology is consistent with what has been observed previously for activated carbons derived from a wide range of sources.[54-56] Indeed, it is now generally accepted that all activated carbons generated via KOH activation possess comparable morphology and that the starting precursor material has little influence on the morphology.

To assess the carbon purity (i.e., lack of inorganic matter) of precursor materials and activated carbons and to assess their thermal stability, we performed thermogravimetric analysis under flowing air conditions. For the sawdust hydrochar and polypyrrole, and all

activated carbons (Supporting Figure S3), there is an initial mass loss of 2 – 5 wt% below 300 ^{o}C, which is attributable to loss of water or volatiles. This is followed by further mass loss, due to carbon burn off, between ca. 300 ^{o}C and 800 ^{o}C for the precursor materials, and ca. 400 ^{o}C and 620 ^{o}C for the activated carbons. The precursor materials have no residual mass, which confirms that they are fully carbonaceous, while the activated carbons had very low residual matter after thermal treatment in air, which also confirms their carbonaceous nature. The elemental composition of the precursors (polypyrrole, raw sawdust and sawdust-derived hydrochar) and activated carbons derived from pre-mixed precursors are given in Table 1. We firstly note that the precursors differ in their O/C ratio, i.e., 0.672 (polypyrrole), 0.773 (raw sawdust) and 0.483 for sawdust hydrochar. The C content of the activated carbons increases compared to that of the precursors, accompanied with decrease in the N, H and O content. When polypyrrole is subjected to activation (sample PPY4800), the carbon content rises from 44.5 to 87 wt%. In contrast, the N content (wt%) and H content (wt%) decreases, respectively, from 12.6 and 3.0 to 0.9 and by 0.2. On activation of the raw sawdust (sample SD4800D), the C content increases from 46.4 wt% to 85.8 wt% and the H content of 5.8 wt% is virtually all removed. Hydrothermal carbonisation of the sawdust to hydrochar increases the C content from 46.4 wt% to 57.4 wt% but with no change in the H content meaning that the O content reduces from 47.8 to 37 wt%. Activation of the hydrochar (sample SD4800) increases the C content to 89.7 wt% and virtually all the H is removed. All the activated carbons, regardless of the precursor, have C content of between 83 and 90 wt%. It is noteworthy that a higher PPY content in the pre-mixed precursor results in greater amounts of N in the activated carbons with the N content ranging between 0.5 and 1.6 wt%. The overall picture that emerges from the elemental composition data in Table 1 is that the activated carbons, regardless of the nature of the pre-mixed precursor they are derived from, have comparable C, H and O content. Furthermore, for both sets of samples, the N content

remains low but slightly increases for samples prepared from pre-mixed precursors with high amount of polypyrrole.

Table 1. Elemental composition of precursors (polypyrole, raw sawdust and sawdust-derived hydrochar) and activated carbons derived from pre-mixed precursors.

Sample	C [%]	H [%]	N [%]	O [%]	(O/C)[a]
Polypyrrole [b]	44.5	3.0	12.6		
PPY4800	87.0	0.2	0.9	11.9	0.103
Raw Sawdust	46.4	5.8	0	47.8	0.773
SD4800D	85.8	0.3	0	13.9	0.122
Sawdust hydrochar	57.4	5.6	0	37.0	0.483
SD4800	89.7	0.1	0	10.3	0.086
PPYSD134800	89.0	0	0.6	10.4	0.088
PPYSD124800	87.8	0	0.8	11.4	0.097
PPYSD114800	87.6	0.1	1.0	11.3	0.097
PPYSD214800	84.5	0	1.2	14.3	0.127
PPYH134800	83.8	0.2	0.5	15.5	0.140
PPYH124800	83.0	0	1.2	15.8	0.143
PPYH114800	87.8	0	1.6	10.6	0.090
PPYH214800	87.0	0	1.6	11.4	0.098

[a]Atomic ratio. [b]Nominal O content of 39.9% obtained as O = 100-C-H-N, which gives O/C ratio of 0.672.

3.2 Textural Properties and Porosity

The nitrogen sorption isotherms and corresponding pore size distribution (PSD) curves for the PPYSD*xyx*t set of samples, the PPY-only derived sample (PPY4800) and raw sawdust (SD) only derived sample (SD4800D), are shown in Figure 1. It is noteworthy that both the PPY-only derived sample (PPY4800) and raw sawdust (SD) only derived sample

(SD4800D) exhibit isotherms that are typical of predominantly mesoporous materials (Figure 1A), which is consistent with previous reports.[33,49] Based on this early data, we propose that the proportion of mesoporosity generated in the activated carbons, and thus the ease of activation, is related to the O/C ratio in the precursors. In this regard, PPY and raw sawdust are readily activated and generate significant mesoporosity due their relatively high O/C ratio of 0.672 and 0.773, respectively. Given that all the PPYSD*xyx*t mixed precursor samples were prepared under similar conditions, the expectation was that they would all exhibit mesoporous characteristics similar to those of PPY4800 and SD4800D. It is therefore interesting to note that not all the isotherms in Figure 1A are indicative of the samples being predominantly mesoporous, and in any case some of the isotherms differ significantly from those of PPY4800 and SD4800D. In particular, the sample made from a 1:3 mixture of PPY and SD (i.e., PPYSD134800) tends towards being more microporous and exhibits a relatively sharp adsorption knee. This clearly indicates that the nature of the precursor mixture can significantly affect the micropore/mesopore proportions in the activated carbons. Samples prepared from 1:1, 1:2 and 2:1 mixture of PPY and SD (PPYSD114800, PPYSD124800 and PPYSD214800) show only moderate mesoporosity that is intermediate between that of the PPY4800 and SD4800 samples and that of the sample derived from a 1:3 PPY/SD mixture. It therefore appears that, for activation at 800 ^{o}C and KOH/precursor ratio of 4, mixing of polypyrrole and raw sawdust in the precursor mix reduces the level of mesoporosity, and that the extent of the reduction is greatest at greater differences in the relative amounts of each precursor (i.e., PPY/SD ratio of 1:3). We interpret the decrease in mesoporosity as being an indication of greater resistance to activation by the 1:3 pre-mixture. The greater resistance may arise from formation of composites between the polypyrrole and the components of sawdust, namely lignin, cellulose and hemi-cellulose. Such composites are known to exist and are considered to be mixtures wherein either of the components

'dissolves' into the other to form stable formations held together by hydrogen bonds.[56-58] Such an arrangement may be best achieved with a 1:3 mixture where there is an excess (solvent) of one component, while the other of lower amounts acts as 'solute'. It is likely that such composites are formed during the slow heating rate (3°/min) considering that the melting point of polypyrrole is lower than that of KOH. No significant activation reactions (i.e., interactions between precursor and KOH) are expected to occur at temperatures below 500 °C. It is therefore possible that composites containing woody material and PPY are formed prior to the activation process, and that such composites are more resistant to activation than either of PPY or SD, and that they are best formed at PPY:SD ratio of 1:3.

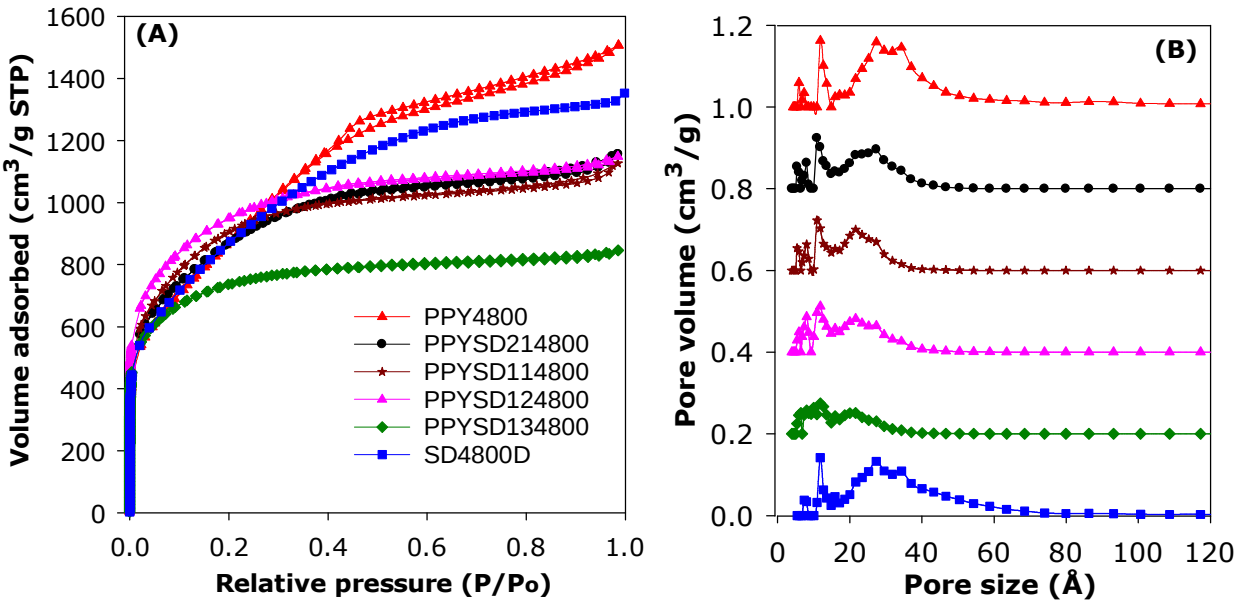

Figure 1. (A) Nitrogen sorption isotherms and (B) pore size distribution curves of single precursor samples, PPY4800 (polypyrole, PPY) and SD4800D (raw sawdust, SD), and carbons derived from pre-mixed precursors containing PPY and SD at various weight ratios.

The pore size distribution of the PPY/SD carbons is shown in Figure 1B, and the pore size maxima values obtained from the curves are given in Supporting Table S1. The PPY-only (PPY4800) and sawdust-only (SD4800D) derived samples exhibit bimodal pore size

distribution with a small proportion of micropores centred at ca. 12 Å, and a much larger proportion of mesopores centered at ca. 30 Å. However, for pre-mix samples, the size of mesopores varies depending on the PPY:SD ratio. The sample made from a 1:3 mixture of PPY and SD (PPYSD134800) has a relatively smaller proportion of mesopores centred at 21 Å, which is consistent with the observation that the sample tends towards being microporous. Indeed, only a small proportion of pores in this sample are larger than 20 Å. For samples PPYSD124800 and PPYSD114800, the mesopores are slightly larger (22 Å), while for sample PPYSD214800 there is a larger proportion of wider (i.e., centered at 25 Å) mesopores. The variation in proportion and size of mesopores confirms that the nature of the precursor mix significantly affects the size of pores generated in the activated carbons. Therefore, in general, for activation at 800 ^{o}C and KOH/precursor ratio of 4, the addition of greater amounts of sawdust to the precursor mix reduces the size of pores generated towards being predominantly in the supermicropore range.

The textural parameters of the activated carbons are summarised in Table 2. The PPY-only derived sample (PPY4800) has surface area of 2965 m^2g^{-1} and pore volume of 2.34 cm^3g^{-1}, while the SD-only derived sample (SD4800D) has surface area of 2980 m^2g^{-1} and pore volume of 2.1 cm^3g^{-1}. All the PPY/SD carbons possess high or ultra-high surface area, which ranges between 2740 and 3500 m^2g^{-1}, and pore volume in the range 1.3 – 1.8 cm^3g^{-1}. The highest surface area for a PPY/SD sample is for PPYSD124800 (3477 m^2g^{-1}) followed by PPYSD114800 (3279 m^2g^{-1}), and it is noteworthy that the surface area of these samples is higher than that of either PPY-only (2965 m^2g^{-1}) or SD-only (2980 m^2g^{-1}) derived carbons. The PPY/SD sample that tends towards being microporous (PPYSD134800) has lower surface area of 2739 m^2g^{-1}, which is lower than that of PPY-only (2965 m^2g^{-1}) or SD-only (2980 m^2g^{-1}) derived carbons. However, in all cases the pore volume of the PPY/SD samples (1.3 – 1.8 cm^3g^{-1}) is lower than that of PPY-only (2.3 cm^3g^{-1}) or SD-only (2.1 cm^3g^{-}

[1]) derived carbons. The greatest reductions in pore volume are for the more microporous PPYSD134800 sample. As shown in Table 2, the highest microporosity (ca. 50% of both pore volume and surface area) is exhibited by sample PPYSD134800. The sample prepared at PPY:SD ratio of 1:2 also exhibits considerable microporosity (ca. 35%). As shown in Table 2, the proportion of volume arising from mesopores (referred to as mesoporosity) increases with increasing amount of polypyrrole in the pre-mix precursor in the range 53 – 90%. Indeed, the most mesoporous PPY/SD sample (PPYSD214800) has 90% of pore volume arising from mesopores, which is comparable to that of PPY-only (92%) or SD-only (86%) derived carbons.

Table 2. Textural properties, excess and total hydrogen uptake of activated carbons derived from single precursors (polypyrrole, raw sawdust and sawdust-derived hydrochar) or pre-mixed mixtures of the precursors.

Sample	Surface area[a] (m^2g^{-1})	Pore volume[b] (cm^3g^{-1})	V_{mes}[c] (%)	H_2 uptake (wt%)[d] 1 bar	20 bar	40 bar	100 bar
PPY4800	2965 (287)	2.34 (0.18)	92	2.2	6.4 (4.9)	8.1 (5.1)	10.9
SD4800D	2980 (478)	2.10 (0.30)	86	2.5	6.3 (5.0)	7.9 (5.2)	
SD4800	2783 (694)	1.80 (0.36)	80	2.4	6.1 (5.0)	7.3 (5.2)	
PPYSD134800	2739 (1562)	1.31 (0.62)	53				
PPYSD124800	3477 (1356)	1.78 (0.62)	65	3.6	7.5 (6.3)	8.9 (6.6)	11.1
PPYSD114800	3279 (1015)	1.70 (0.39)	77	2.7	6.5 (5.4)	7.8 (5.6)	9.8
PPYSD214800	3085 (452)	1.76 (0.18)	90	2.7	6.4 (5.3)	7.8 (5.5)	9.8
PPYH134800	1828 (1468)	0.83 (0.59)	29				
PPYH124800	2227 (1569)	1.04 (0.62)	40				
PPYH114800	3815 (1377)	2.18 (0.66)	70	3.3	8.1 (6.7)	10.0 (7.1)	12.6
PPYH214800	3583 (887)	1.97 (0.35)	82	3.0	7.3 (6.0)	8.8 (6.2)	11.1

[a]The values in the parenthesis are micropore surface area. [b]The values in the parenthesis are micropore volume. [c]Proportion of pore volume arising from mesopores. [d]The values in parenthesis are the excess hydrogen uptake.

The porosity data discussed above indicates that addition of sawdust to polypyrrole acts to reduce the overall mesoporosity of the resulting activated carbons. Several previous studies have hinted that the extent of activation of a carbonaceous precursor may be related to elemental composition. To test and clarify this hypothesis further, we used pre-mixed precursors containing PPY and sawdust hydrochar, which has a O/C ratio of 0.483. The expectation was that the presence of hydrochar in the pre-mixed precursor would act to limit the mesoporosity to an even greater extent (compared to PPY/SD samples) due to the lower O/C ratio of the hydrochar compared to sawdust and the fact that the hydrochar is not expected to form any stable formations in a manner similar to the PPY/sawdust composites as discussed above. The nitrogen sorption isotherms of the PPYH*xyx*t carbons are shown in Figure 2A, and the corresponding pore size distribution (PSD) curves and are shown in Figure 2B. The nitrogen sorption isotherms suggest that, in general, the porosity of the PPY/H carbons is lower than that of PPY/SD equivalents. The isotherms show great variability between the samples, but there are also some apparent trends. The amount of nitrogen adsorbed appears to be related to the amount of PPY present in the precursor mix, i.e., decreases in the order PPYH114800 ~ PPYH214800 > PPYH124800 > PPYH134800. It appears therefore that the addition of sawdust hydrochar to the precursor mix reduces the extent of porosity/mesoporosity generated to the extent that samples PPYH124800 and PPYH134800 have isotherms that suggest that they are significantly microporous. This trend confirms that the nature of the precursor significantly affects the micropore/mesopore mix in the activated carbons, and is also consistent with the lower O/C ratio of the hydrochar.

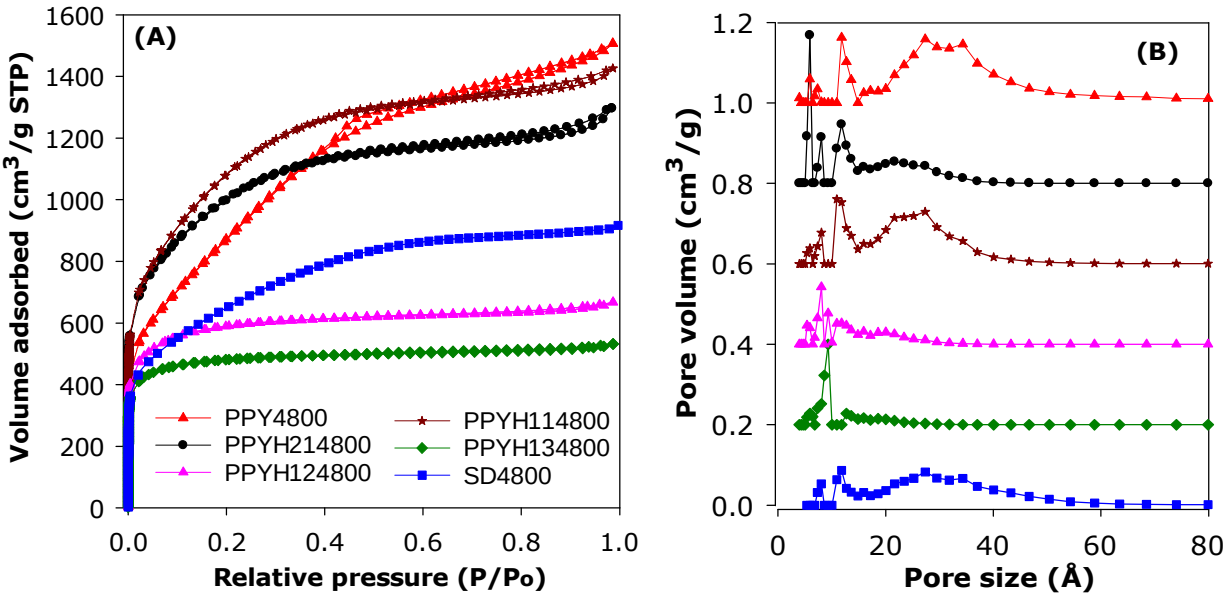

Figure 2. (A) Nitrogen sorption isotherms and (B) pore size distribution curves of single precursor, PPY4800 (polypyrole, PPY) and SD4800 (raw sawdust hydrochar, H), and carbons derived from pre-mixed precursors containing PPY and H at various weight ratios.

The pore size distributions of the PPY/H carbons are shown in Figure 2B, and the pore size maxima values obtained from the curves are given in supporting Table S1. The pore size distribution of the PPY/H carbons differs quite significantly from that of PPY4800 and SD4800. Sample PPYH134800, PPYH124800 and PPYH214800 are dominated by micropores of size between 9 and 16 Å. Indeed, the pore size of these samples prepared from a PPY/H precursor mix ratio of 1:2. 2:1 or 1:3 is dominated by micropores with hardly any pores larger than 20 Å. On the other hand, sample PPYH114800 contains a large proportion of pores centre at 25 Å. In general, the presence of mesopores in the PPY/H set of samples can be related to the amount of PPY in the precursor mix, and the size of the mesopores varies depending on the PPY:H ratio.

The textural parameters of the PPY/H carbons are summarised in Table 2. All the carbons possess moderate, high or ultra-high surface area, which ranges between 1800 and 3815 m^2g^{-1}, and pore volume in the range 0.8 – 2.3 cm^3g^{-1}. The highest surface area is for

PPYH114800 (3815 m^2g^{-1}) followed by PPYH214800 (3583 m^2g^{-1}). The addition of sawdust hydrochar to the precursor mix at non-equal amounts (i.e., ratios 1:2. 2:1 and 1:3) has a significant effect of the total surface area except for sample PPYH214800. However, in general, the addition of sawdust hydrochar to the precursor mix reduces the pore volume, with the greatest reductions being for samples prepared from 1:2 or 1:3 PPY:H ratios (samples PPYH124800 and PPYH134800, respectively). The volume arising from mesopores increases with the amount of PPY in the precursor. This means that increase in the amount of sawdust hydrochar in the precursor mix reduces the proportion of mesopores. This is consistent with our proposal that the sawdust hydrochar has a lower O/C ratio and therefore expected to be more resistant to activation compared to polypyrrole.

The pore channel ordering of both sets of carbons can be observed using TEM imaging. Both sets of carbons ((Supporting Figure S4 and S5) exhibit wormhole type pore channel ordering that is typical of activated carbons. The TEM images for both sets of activated carbons show no significant evidence of the presence of graphitic domains, which is consistent with the high porosity observed.

The effect of elemental composition, and in particular the O/C ratio, on the activation of various precursors and generation of mesoporosity may be clarified by considering the behaviour of a number of carbonaceous matter with varying O/C ratio. In this regard, we compared the porosity of PPY4800, SD4800D and SD4800 to that of equivalent activated carbons derived from hydrochars of lignin[54] and Jujun grass,[42] and carbonaceous matter obtained from biomass via carbonisation in the presence of air (i.e., via flash carbonisation that involves a flame).[46,48] The selected carbonaceous precursors differ significantly in their elemental (C, H, O) compositions and O/C ratio as shown in supporting Table S2. The O/C ratio varies between 0.185 and 0.773 in the order raw sawdust > PPY > Jujun grass hydrochar > sawdust hydrochar > lignin hydrochar > flash carbonised sawdust > CNL1 carbon. All the

carbonaceous precursors were similarly activated (i.e., at 800 °C and KOH/precursor ratio of 4). We then compared the nitrogen sorption isotherms and pore size distributions (Figure 3) and textural properties (Table 3) of the resulting activated carbons. The textural data very clearly shows that there is a relationship between the O/C ratio of the precursor and extent of mesoporosity generated in the activated carbons. The amount of nitrogen adsorbed (Figure 3B) closely follows the trend in O/C ratio. The shapes of the isotherms also indicate that carbonaceous precursors with high O/C ratio generate activated carbons (e.g. PPY4800 and SD4800D) with 'gentle knees' that have significant adsorption at relative pressure above P/Po = 2. On the other hand, the isotherms of activated carbons obtained from precursors with low O/C ratio (e.g., CNL1-4800 and ACSD-4800) have 'sharp knees' with hardly any increase in adsorption above P/Po = 0.2.

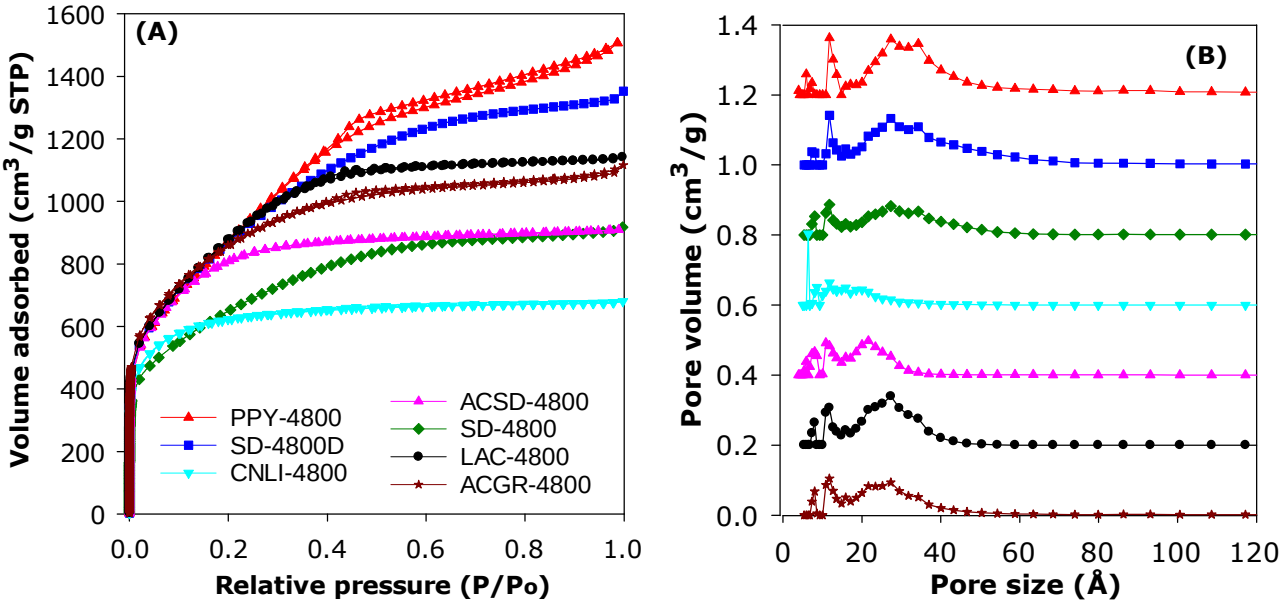

Figure 3. (A) Nitrogen sorption isotherms and (B) pore size distribution curves of activated carbons derived from polypyrrole (PPY-4800), raw sawdust SD-4800D), sawdust hydrochar (SD-4800), CNL1 carbon (CNL1-4800), flash air carbonized sawdust (ACSD-4800), lignin hydrochar (LAC-4800) and Jujun grass hydrochar (ACGR-4800). All the activated carbons were prepared at activation temperature of 800 °C and KOH/precursor ratio of 4.

Table 3. Textural properties and O/C ratio of activated carbons derived from polypyrrole (PPY-4800), raw sawdust SD-4800D), sawdust hydrochar (SD-4800), CNL1 carbon (CNL1-4800), flash air carbonized sawdust (ACSD-4800), lignin hydrochar (LAC-4800) and Jujun grass hydrochar (ACGR-4800). All the activated carbons were prepared at activation temperature of 800 ^{o}C and KOH/precursor ratio of 4.

Sample	Precursor O/C ratio	Surface area[a] (m^2 g^{-1})	*Meso* SA (%)	Pore volume[b] (cm^3 g^{-1})	*Meso* PV (%)	Pore size[c] (Å)
PPY4800	0.672	2965 (287)	90	2.34 (0.18)	92	12/30
SD4800D	0.773	2980 (478)	84	2.10 (0.30)	86	12/29
SD4800	0.483	2783 (694)	75	1.80 (0.36)	80	11/27
CNL1-4800	0.185	2183 (1886)	14	1.05 (0.84)	20	6.5/8.5/16
ACSD-4800	0.251	2610 (1892)	28	1.15 (0.74)	36	6/8/10/16
LAC-4800	0.319	3235 (1978)	39	1.77 (0.93)	47	8/11/27
ACGR-4800	0.519	2957 (1578)	47	1.72 (0.75)	56	8/12/27

The values in the parenthesis refer to: [a]micropore surface area and [b]micropore volume. [c]pore size distribution maxima obtained from NLDFT analysis. *Meso* SA and *Meso* PV are proportion (%) of surface area and pore volume, respectively, arising from mesopores.

As discussed above, precursors with higher O/C ratio generate activated carbons (PPY4800 and SD4800) that are essentially mesoporous (i.e., easy to activate), while low O/C ratio precursors that are resistant to activation tend to yield carbons that are more microporous (CNL1-4800 and ACSD-4800). The level of mesoporosity is a measure of the ease of activation of the precursors; high O/C ratio precursors are readily activated (or more activated with larger pores) while low O/C precursors are more resistant to activation with KOH and therefore mainly possess micropores. Thus, sample CNL1-4800 is almost entirely microporous (i.e., proportion of micropore volume or microporosity is 84%), while on the other end of the scale samples PPY4800 and SD4800D have microporosity of only 10 – 16%. Indeed, CNL1-4800 has hardly any mesopores, while PPY4800 has virtually no micropores (Figure 3B) because of their vastly different O/C ratio (0.672 for PPY vs 0.185

for CNL1 carbon). We, furthermore, note that an attempt to directly activate cellulose acetate, which has a high O/C ratio of 0.93, failed as no carbon yield was obtained. We interpret the lack of any yield as an indication of complete burn-off of the cellulose acetate due to being readily activateable. These observations are consistent with our explanations for the trends in the porosity of the carbons obtained from the pre-mixed precursors and offer new insights on the possibility of tailoring the porosity of activated carbons by simple selection of single or a mix of precursors. Regarding the effect of high O/C ratio, it is likely that higher O content signifies the presence of a greater proportion of O-containing polar functional groups that improve the ease of activation. In contrast, low O/C ratio is associated with presence of stable carbon forms that are resistant to activation.[45]

To further probe the content of oxygen in the precursor materials, and to have independent verification of the O/C ratio, we performed X-ray photoelectron spectroscopy (XPS). Wide XPS scans were used to quantify the elemental composition of three precursor samples, namely sawdust hydrochar, polypyrrole and CNL1 carbon. For sawdust hydrochar and CNL1 carbon, only O and C were present in detectable quantities (Supporting Figure S6). While as expected polypyrrole also contained N in addition to O and C. Regarding the C and O content, it is interesting to note that both the sawdust hydrochar and polypyrrole contain a high amount of O, while the CNL1 carbon has a much lower O content. These findings are exactly in line with the elemental composition reported in Table 1. Indeed, the oxygen contents (wt%) on the surface estimated from the XPS spectra are comparable to those obtained via elemental (i.e., CHN) analysis, being 33.7% (sawdust hydrochar), 34.5% (polypyrrole) and 17.9% (CNL1 carbon). These values are particularly important in confirming that the polypyrrole used in this study contained a significant amount of O, which is consistent with previous studies on similar polymers.[59-61] The nature of the precursor materials and their oxygen content was further explored by performing temperature

programmed desorption (TPD). TPD is a useful tool as it enables tracking of any desorbed CO_2, which comes from functional groups such as carboxylic acids, lactones and anhydrides that are less thermally stable, and CO from more thermally stable carbonyls, quinonic or phenolic groups.[62] Desorption of CO_2 occurs between 150 and 550 ^oC, while CO is desorbed at higher temperature of 400 - 950 ^oC. The TPD profiles obtained for the selected precursor materials (Supporting Figure S7) are consistent with those previously reported for carbonaceous matter.[62] More importantly, the TPD profiles allow an independent (from elemental analysis data) verification of the oxygen content and O/C ratio. The oxygen content estimated from the TPD profiles (i.e., 37.7% (sawdust hydrochar), 38.4% (polypyrrole) and 18.5% (CNL1 carbon)) was comparable to that from CHN elemental analysis (Table 1), which was added verification of the O/C ratio of the precursor materials.

3.3 Hydrogen Storage

To date, the best performing carbon-based hydrogen storage materials are zeolite-templated carbons,[11,14,15,63-66] carbide-derived carbons (CDCs)[67] and activated carbons.[13,29-34,68,69] The hydrogen storage capacity of the PPY/SD and PPY/H carbons was determined at -196 ^oC and in the pressure range 0 – 100 bar, with particular emphasis on uptake at 40 bar. The emphasis on uptake at 40 bar was informed by two reasons; (i) cryo-storage at such a pressure has recently received strong consideration as being viable for low-pressure vehicular hydrogen storage,[70-73] and (ii) the excess hydrogen uptake under cryogenic conditions tends to be at a maximum at ca. 40 bar and is therefore a good indicator of a solid's performance in storing hydrogen once packed into a confined space compared to the empty space. For porous materials, it is known that the cryogenic hydrogen storage capacity requires high surface area.[74-78] Therefore, in this study, we only assessed the hydrogen uptake of PPY/SD and PPY/H carbons with surface area higher than 3000 m^2g^{-1}.

Our hydrogen uptake measurements, obtained using a Hiden XEMIS analyser, were set up to determine the excess storage capacity from which the total hydrogen stored at any given pressure may be calculated using established procedures (further details are in the Supporting Information). The hydrogen uptake is presented as wt% based on the dry material (carbon) weight. We firstly note that the excess hydrogen uptake of the single precursor samples (PPY4800, SD4800D and SD4800) is quite similar (Supporting Figure S8 and Table 2). Thus, rather than use the hydrogen storage capacity of all three samples as a baseline for our discussions below, we instead only use the uptake PPY4800 as it is the common precursor in all the samples. The excess hydrogen uptake isotherms of PPY4800 along with those of the PPY/SD and PPY/H carbons are presented in Figure 4, and Table 2 summarises the hydrogen storage capacity for both sets of carbons at 1, 20 and 40 bar. The hydrogen uptake isotherms are completely reversible with no hysteresis in the pressure range 0 – 100 bar. At 1 bar, the single precursor samples store 2.2 – 2.5 wt% hydrogen. For the PPY/SD samples, the hydrogen storage capacity at 1 bar is between 2.7 and 3.6 wt%, while for the PPY/H samples it is in the range of 3.0 to 3.3 wt%. Uptake of 2.7 to 3.6 wt% at 1 bar for the pre-mix samples is very high and amongst the highest ever reported for carbons. The hydrogen uptake at pressures between 20 bar and 40 bar is often used as measure of a carbon's efficiency for hydrogen storage under 'low to moderate' pressure. As shown in Figure 4 and Table 2, at 20 bar, the excess hydrogen uptake of the pre-mix carbons varies between 5.3 and 6.7 wt% compared to ca. 5.0 wt% for the single precursor samples. This represents a 34% increase in excess hydrogen storage capacity for sample PPYH114800 (6.7 wt%) compared to PPY4800 (4.9 wt%) and SD4800 (5.0 wt%). The excess hydrogen uptake at 20 bar appears to be determined by several factors, namely, (i) the total surface area, with uptake of 6.7 wt% for the highest surface area sample (PPYH114800); (ii) the trend in micropore surface area, which decreases in the same manner as the hydrogen uptake, and (iii) the PPY:SD or PPY:H ratio in the precursor mix, with

greater amounts of sawdust or hydrochar appearing to favour higher hydrogen uptake, which may simply be due to the fact that greater amounts of sawdust or hydrochar in the precursor mix lead to higher levels of microporosity.

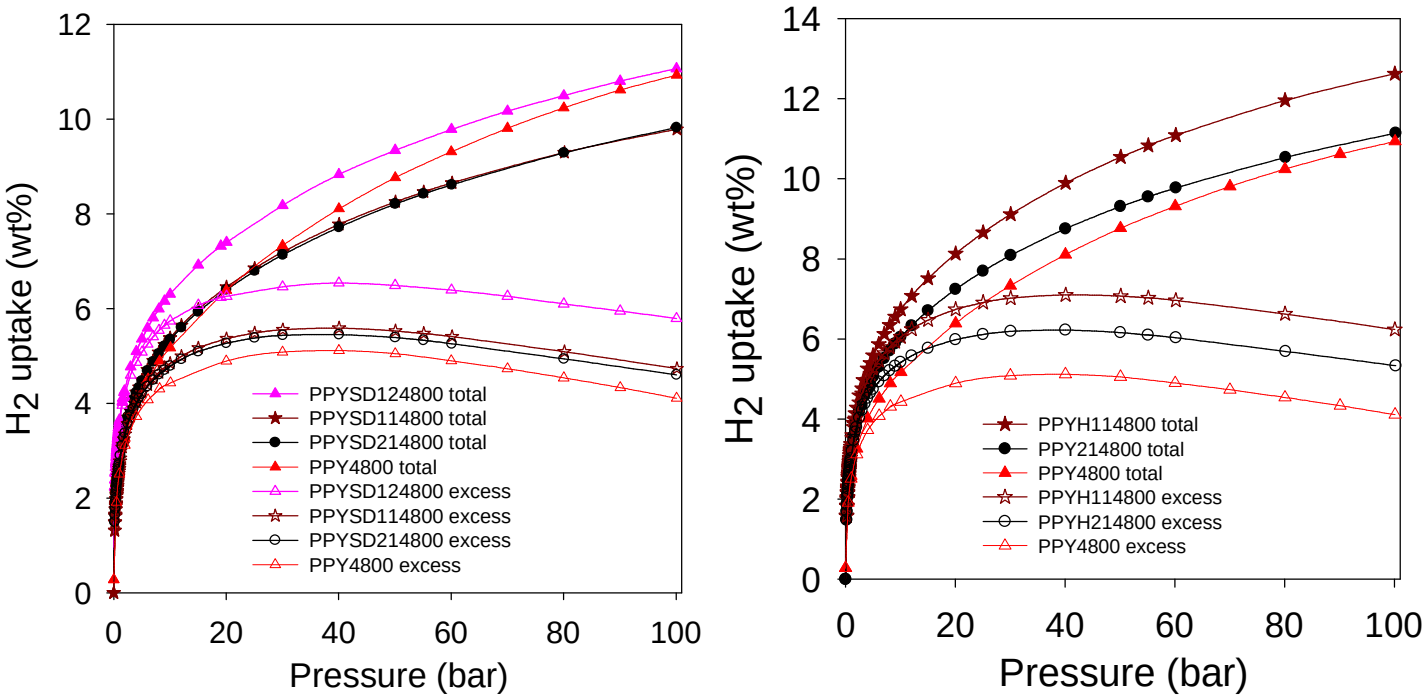

Figure 4. Hydrogen uptake isotherms of single precursor PPY4800 (polypyrole, PPY) and (left panel) PPY/SD carbons derived from pre-mixed precursors containing PPY and raw sawdust (SD), and (right panel) PPY/H carbons derived from pre-mixed precursors containing PPY and sawdust hydrochar (H) at various weight ratios.

As shown in Figure 4, the carbons achieve their maximum excess uptake at ca. 40 bar. The excess uptake at 40 bar is summarised in Table 2 and generally follows the trends discussed above for uptake at 20 bar. The highest excess uptake at 40 bar for the pre-mix precursor samples is 7.1 wt% for sample PPYH114800, while the lowest is 5.5 wt% for PPYSD214800. This means that all the tested pre-mix precursor samples outperform the single precursor uptake of ca. 5.2 wt%., with the best performance representing an improvement in storage capacity of 37%. For the pre-mix precursor samples, the total hydrogen uptake at 20 bar is in the range 6.4 to 8.1 wt%. Hydrogen uptake of 8.1 wt% for sample PPYH114800, which is an improvement of ca. 30% over

the single precursor samples, is very impressive and compares favourably with the best carbons reported so far. For context, the best reported hydrogen uptake values under similar conditions (-196 ^{o}C and 20 bar) are; 7.3 wt% for polypyrrrole-only derived compactivated carbons,[29] 7.08 wt% for a carbon that was both physically and chemically activated,[69] 7.1 wt%, for a sawdust-derived compactivated carbon,[29] 7.3 wt% for a zeolite templated carbon,[14] 8.2 and 9.4 wt% for activated carbon derived from hydrochar of, respectively, fresh and smoked cigarette butts,[66] and 8.1 wt% for oxygen-rich activated carbon derived from cellulose acetate hydrochar.[13] It is therefore clear that the use of mixed precursors offers carbons with hydrogen uptake that outperform all previously reported materials generated singly from polypyrrole or sawdust. At 40 bar, the total hydrogen uptake is in the range 7.8 to 10.0 wt%. A total hydrogen uptake of up to 10.0 wt% at 40 bar, and 12.6 wt at 100 bar for sample PPYH114800 is all round very impressive and far outperforms the carbons prepared singly from polypyrrole or sawdust (Table 2).

A positive consequence of the lower mesoporosity of the pre-mix precursor samples is that their packing density rises above that of the single precursor carbons. For most porous materials, packing density is inversely proportional to pore volume, especially pore volume airing from large pores (mesopores and macropores). The packing density of porous solids is very important with respect to their use as hydrogen stores as it determines how much is stored in any confined space (e.g., storage tank) that is packed full with the material. Thus the volumetric storage capacity, which is as important as the gravimetric capacity, depends critically on the packing density. For this reason, it is necessary that materials achieve both gravimetric and volumetric storage targets. An example of such targets are those of the United States Department of Energy (DOE) that require achievement of a set gravimetric and volumetric uptake. The packing density of the present samples (Table S1) was determined from pellets compacted in a 1.3 cm die for ca. 5 min at 7 MPa or from the general equation; $d_{carbon} = (1/\rho_s + V_T)^{-1}$, where ρ_s is skeletal density and V_T is total pore volume. The

volumetric storage uptake isotherms computed from the gravimetric uptake and packing density (See Supporting Information) are shown in Figure 5. A combination of greater packing density and better gravimetric uptake means that the volumetric hydrogen storage capacity of the pre-mix carbons is much higher than that of single precursor PPY4800. The volumetric hydrogen uptake of the best performing pre-mix samples (PPYH114800, PPYSD114800 and PPYSD124800) is almost double that of PPY4800 in the pressure range 5 – 100 bar. The pre-mix samples show excellent volumetric hydrogen storage capacity at 20 bar; 25 – 28 g l^{-1} (excess) and 30 – 33 g l^{-1} (total) compared respectively to 17 and 22 g l^{-1} for PPY4800. At 40 bar the uptake is 26 – 30 g l^{-1} (excess) and 36 – 40 g l^{-1} (total), which is much higher than 18 and 28 g l^{-1} for PPY4800.

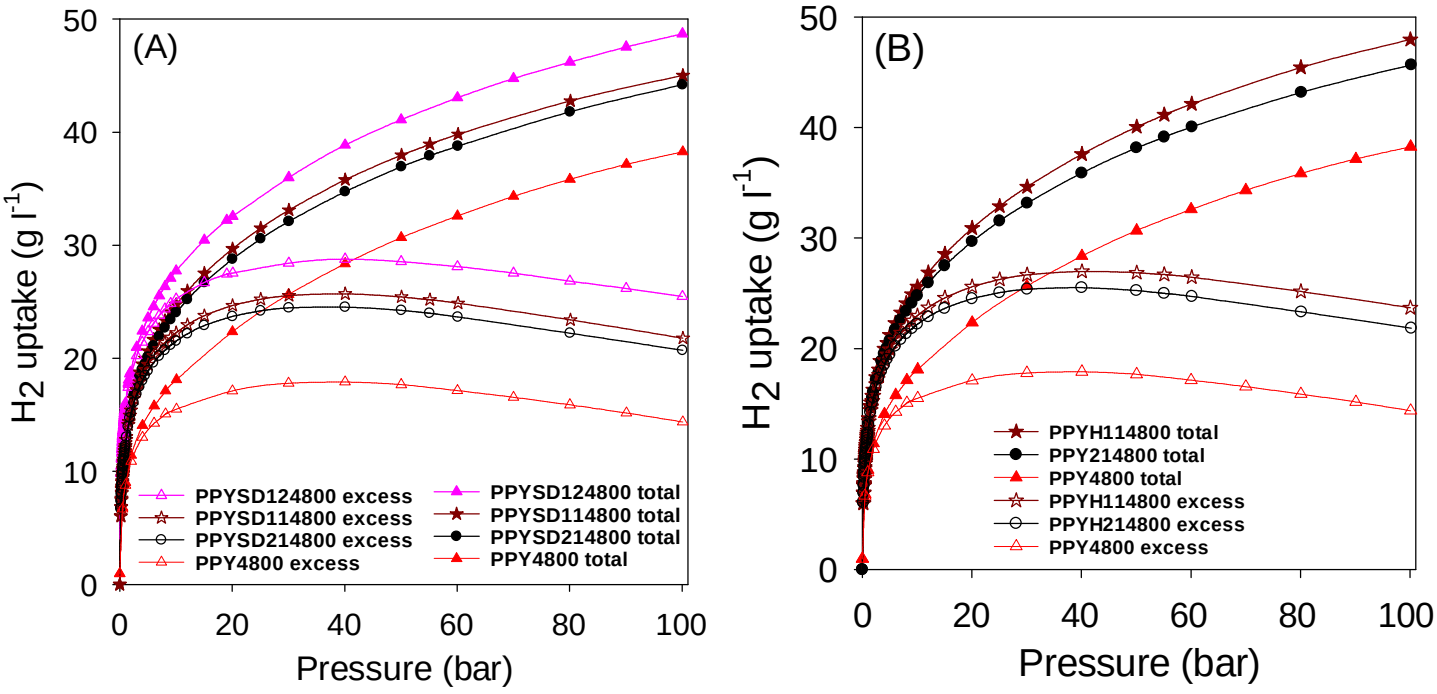

Figure 5. Volumetric hydrogen uptake isotherms of single precursor PPY4800 (polypyrole, PPY) and (A) PPY/SD carbons derived from pre-mixed precursors containing PPY and raw sawdust (SD), and (B) PPY/H carbons derived from pre-mixed precursors containing PPY and sawdust hydrochar (H) at various weight ratios.

It is interesting to compare the hydrogen storage uptake of one of the better performing samples (PPYH114800) with that of current non-carbon benchmark materials such as metal organic frameworks (MOFs). Firstly, we note that at 20 bar, the excess hydrogen storage capacity of PPYH114800 (6.7 wt%) is comparable (Figure 6 and Supporting Table S4) to that of the best metal organic framework (MOFs), namely, NOTT-112 (6.9 wt%),[79] NU-100 (6.8 wt%)[22] and MOF-210 (6.4 wt%),[24] that are considered to be 'record holders' for gravimetric hydrogen storage in porous materials under cryogenic conditions. The total hydrogen uptake of PPYH114800 (8.1 wt%), at 20 bar, is also comparable to NU-100 (8.5 wt%),[22] MOF-210 (8.4 wt%)[24] and NOTT-112 (7.8 wt%).[79] At our target pressure of 40 bar, the total gravimetric hydrogen uptake of PPY114800 (10 wt%), is comparable to NU-100 (10.5 wt%),[22] MOF-210 (11 wt%)[24] and NOTT-112 (9.2 wt%).[79] However, the pre-mix samples do have the advantage of being cheaper, easier to synthesise and also having the attraction of offering valorisation of waste materials such as sawdust.

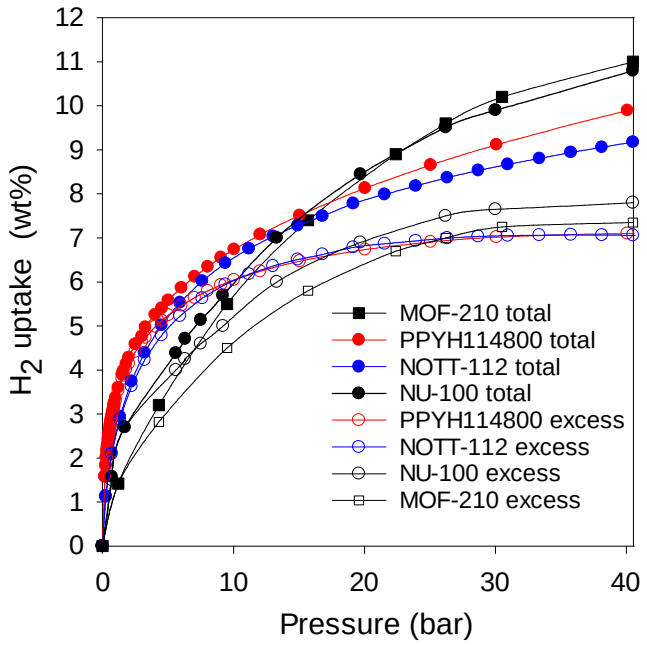

Figure 6. Excess and total gravimetric hydrogen uptake of activated carbon (PPYH114800) derived pre-mixed precursor containing polypyrrole and sawdust hydrochar compared to metal organic frameworks (MOFs); NOTT-112,[79] NU-100,[22] and MOF-210.[24]

The gravimetric uptake of the pre-mix samples, therefore, compares well with that of the best performing MOFs despite the later having much higher surface area and pore volume. As stated above, the volumetric hydrogen uptake of any solid-state storage materials is perhaps more important than the gravimetric uptake. Thus although MOFs have high gravimetric uptake due to their greater surface area and pore volume, the higher porosity also means that they tend to have low packing density. In most reports to date, the volumetric uptake of MOFs is computed using their crystal density rather than packing density.[79-82] The values obtained using crystal density are prone to overestimation as it is not feasible to fill up a container (for example a cylinder) to the extent that the mass-volume ratio in the constrained space is defined by the crystal density. More recently, there are reports that indicate that the actual packing density of MOFs (as defined in this study) is lower (typically ca. 50%) of the crystal density.[83-90] For example, the tap density of MOF-5 was found to be ca. 0.22 g cm^{-3} as opposed to the crystal density of 0.61 g cm^{-3}.[88] We have also shown that the packing density of UiO-66 of 0.57 g cm^{-3} is about half the crystal density of 1.24 g cm^{-3}.[85] Furthermore, unlike for activated carbons,[29] studies also show that compaction of most high surface area MOFs leads to porosity reduction and thus a lowering of hydrogen uptake.[83-90] It is thus likely that the high uptake values obtained for powder samples[22,24,79-82,90] may not be replicated for compacted MOFs.[83-90] We compared the volumetric uptake of the better performing pre-mix samples (PPYH114800 and PPYSD124800), which have a density of 0.38 and 0.44 g cm^{-3}, respectively, with that of benchmark MOFs. As shown in Figure 7 (and Supplementary Table S4), at 20 bar, the benchmark MOFs achieve volumetric hydrogen uptake of 11 – 18 g l^{-1} (calculated based on realistic packing density according to reference 83), compared to 30.8 and 32.6 g l^{-1} for sample PPYH114800 and PPYSD124800, respectively. At 40 bar the MOFs have uptake of 14 – 22 g l^{-1} at 30 bar compared to 38 and 39 g l^{-1} for PPYH114800 and PPYSD124800, respectively. Even when the crystal density is used to compute the volumetric

uptake (Supporting Figure S9 and Table S4), the storage capacity of the MOFs is still lower (MOF-210 and NU-100) or comparable to that of the pre-mix precursor derived samples.

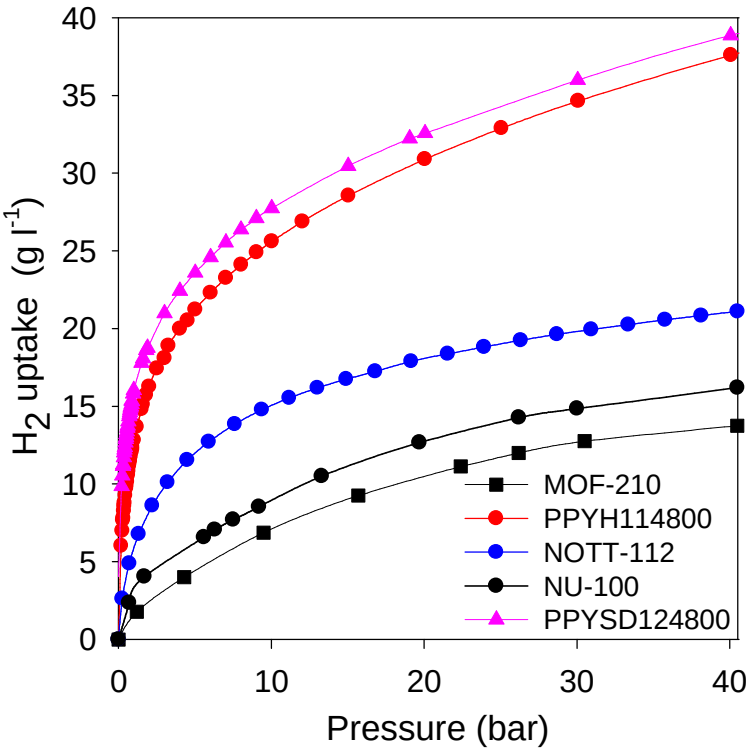

Figure 7. Volumetric hydrogen storage capacity of activated carbons (PPYH114800 and PPYSD124800) derived from pre-mixed precursor containing polypyrrole and sawdust hydrochar or raw sawdust compared to the best performing metal organic frameworks (MOFs); NOTT-112,[75] NU-100,[22] and MOF-210.[24]

Although the total hydrogen uptake (both on a gravimetric and volumetric basis) is a good indicator of hydrogen storage performance, we also need to consider the deliverable hydrogen. We therefore explored the performance of the pre-mix samples under delivery conditions, i.e., deliverable gravimetric and volumetric hydrogen capacity based on pressure swing between 100 bar and 5 bar at 77 K, that have recently been used as viable indicator for vehicular hydrogen storage.[76] We compared the deliverable hydrogen performance of the

pre-mix samples with that of a selection of MOFs (Supporting Table S5)[80] by taking the difference between the total hydrogen uptake at 100 bar and 77 K and at 5 bar and 77 K. The deliverable gravimetric hydrogen capacity of the pre-mix carbon samples, i.e., 5.3 to 7.1 wt%, is higher or comparable to that of the MOFs (2 – 6.9 wt%, except for NU-1103 with 10.1 wt%). Indeed, the deliverable capacity of some of the pre-mix carbons matches or surpasses that of MOFs recently identified as having best deliverable hydrogen storage capacity.[80] The deliverable volumetric uptake of the pre-mix samples is 24 - 27 g l^{-1}, which is comparable to that of the best MOFs (17 – 33 g l^{-1}) if the crystal density is used to compute the volumetric uptake for the MOFs.[80] However, as discussed above, use of the crystal density is unrealistic and overestimates the volumetric uptake. It has been suggested that the volumetric uptake based on crystal density should be adjusted by a reduction of 25% to take into account the packing density.[80] The values obtained following 25% reduction (i.e., 13 – 25 g l^{-1}) suggest that the pre-mix samples can outperform the MOFs. If more realistic packing (or tapping) density is used to compute volumetric uptake (Table S5) then deliverable volumetric capacity of the MOFs (9 – 17 g l^{-1}) is significantly lower compared to that of the pre-mix carbon samples.

The uptake of hydrogen at room temperature was also explored for the best performing pre-mix sample (PPYH114800). The excess and total hydrogen uptake at room temperature for sample PPYH114800 is shown in Figure 8 along with that of a commercially available high surface area carbon (sample AX21). As a verification of our hydrogen uptake measurements, it is noteworthy that for sample AX21, the excess uptake at 20 bar is 0.3 wt%, which is similar to what has previously been reported in measurements that utilised volumetric apparatus.[8] The hydrogen uptake of sample PPYH114800 at 20 bar is 0.5 wt%, which is 67% higher than that of AX21. At 100 bar, the excess uptake rises to 0.8 wt% for AX21, and 1.3 wt% for PPYH114800. We attribute the greater uptake of the pre-mix

PPYH114800 sample to its higher surface area. More generally, sample PPYH114800 appears to have very attractive room temperature hydrogen uptake when compared to other forms of porous carbon or non-carbonaceous materials.[8,91,92] The performance of PPYH114800 (i.e., excess hydrogen storage capacity of 1.3 wt% at room temperature and 100 bar is notably high when compared to all previously reported porous material. Indeed, such uptake compares favourably with values of between 0.5 and 1.6 wt% that have previously been reported for some of the best performing state-of-the-art materials but at a higher pressure of 150 bar.[8,91,92] The estimated total hydrogen uptake for PPYH114800 and AX21 is shown in Figure 8. The total uptake, at 20 bar, reaches 0.6 wt% for AX21, and 0.9 wt% for PPYH114800 while at 100 bar it is 2.1 wt% for AX21 and much higher at 3.0 wt for PPYH114800.

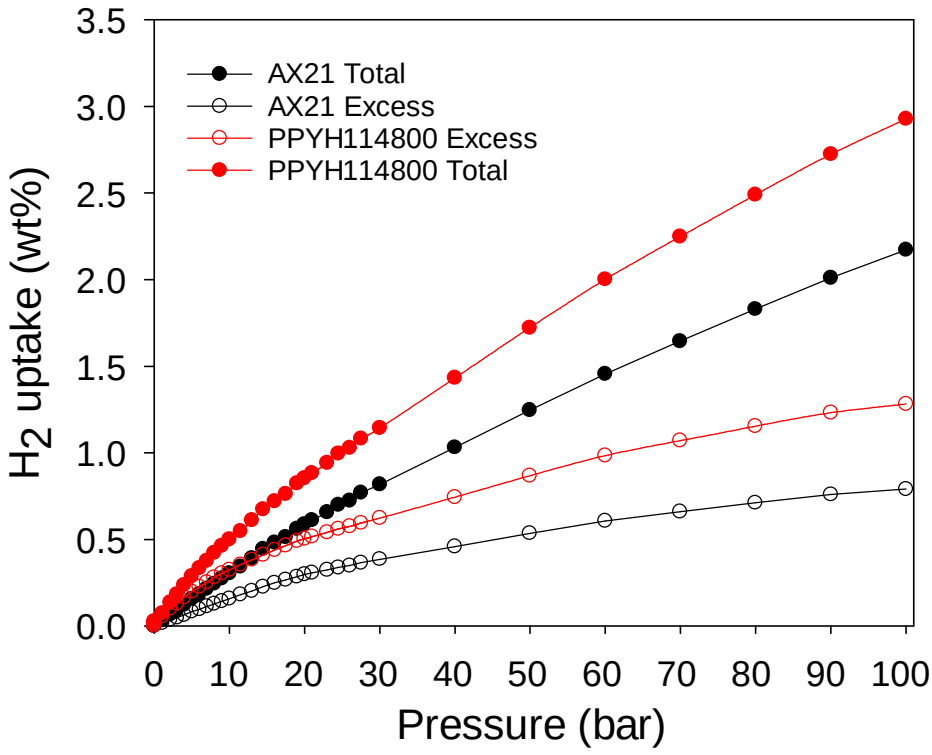

Figure 8. Room temperature hydrogen storage capacity for sample PPYH114800 and a commercially available activated carbon AX21.

3.4 Modulating Porosity at higher levels of Activation

The porosity of activated carbons generated from any given precursor tends to have an optimal level of activation beyond which the surface area reduces. For example, in the case of polypyrrole, the optimal level of activation appears to be a temperature of 800 ^{o}C and KOH/polypyrrole ratio of 4. We have previously shown that increasing the activation temperature above 800 ^{o}C and/or KOH/polypyrrole ratio above 4 reduces the surface area whilst also creating larger pores due to what may be described as 'overactivation'.[33] However, as discussed above for the pre-mix samples, the presence of sawdust hydrochar appears to reduce the extent of mesoporosity. We interpret the reduction in mesoporosity as being due to greater resistance to activation arising from the presence of hydrohar in the precursor mix. We therefore sought to find out whether higher surface area could be achieved (via suppression of 'overactivation') for samples derived from pre-mix precursors activated at greater severity than 800 ^{o}C and KOH/polypyrrole ratio of 4. This was accomplished by activating 1:1 mixture of PPY/SD or PPY/H at 900 ^{o}C and KOH/precursor ratio of 4 or at 800 ^{o}C and KOH/precursor ratio of 5. We then compared the porosity of the resulting carbons with equivalent single precursor (i.e., polypyrrole only) samples as shown in Figure 9 and Table 4. It is clear from the nitrogen sorption isotherms (Figure 9A) that the level of mesoporosity for the pre-mix precursor samples is lower than that of equivalent PPY-only carbons. The pre-mix precursor samples have a sharper sorption knee, and lower adsorption at high partial pressures (P/Po) above 0.8. It is also clear from the PSD curves in Figure 9B that, whilst the PPY-only carbons have a large proportion of pores that are wider than 40 Å, such pores hardly exist for the pre-mix samples as summarised in Table 4. It is noteworthy that whilst the main mesopore maxima for sample PPY5800 is at 35 Å (which is an increase from 30 Å for PPY4800), for sample PPYSD115800 the maxima is at lower pore size of 24 Å. A similar trend is observed for activation at 900 ^{o}C and KOH/precursor ratio of 4, i.e.,

mesopore maxima of 36 Å for PPY4900 compared to 27 Å for PPYSD114900 and PPYH114900. Clearly, the presence of raw sawdust or sawdust hydrochar limits the size of mesopores generated, and therefore enables porosity modulating.

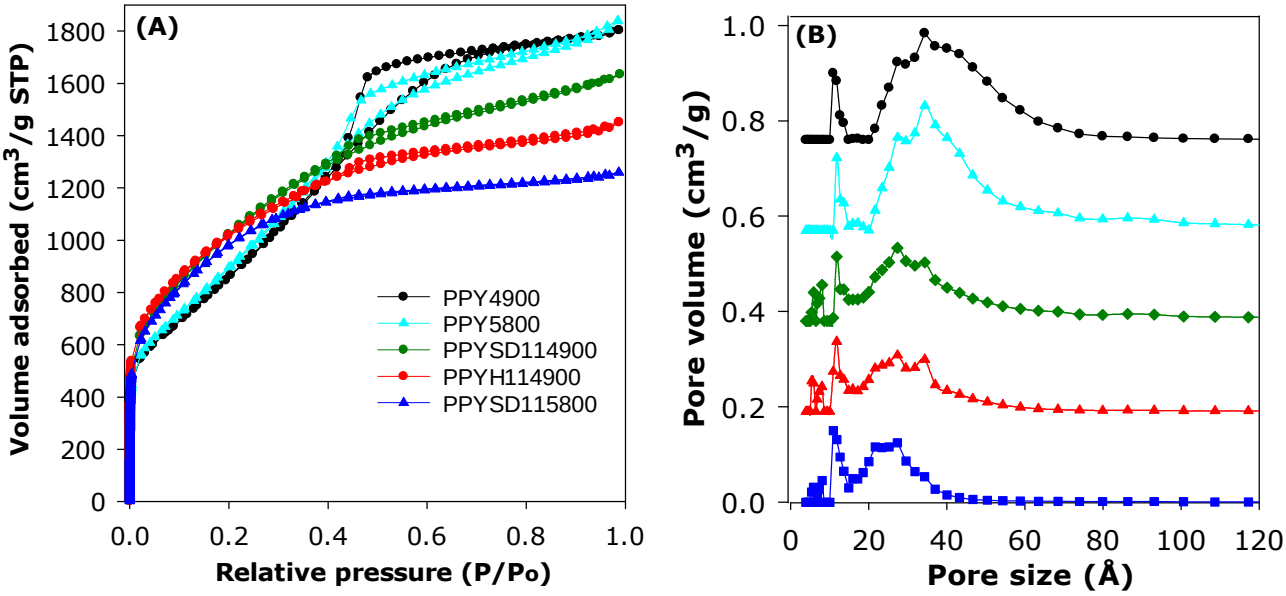

Figure 9. (A) Nitrogen sorption isotherms and (B) pore size distribution curves of activated carbons derived from polypyrrole, or pre-mixed precursors containing polypyrrole and raw sawdust or sawdust-derived hydrochar.

Table 4. Textural properties and hydrogen uptake of activated carbons derived from polypyrrole, or pre-mixed precursors of polypyrrole and raw sawdust or sawdust hydrochar.

Sample	Surface area (m^2g^{-1})	Pore volume (cm^3g^{-1})	Pore size[a] (Å)	Packing density (gcm^{-3})	H_2 uptake (wt%)[b] 1 bar	20 bar	40 bar	100 bar
PPY4800	2965	2.34	12/30	0.35	2.2	6.4 (4.9)	8.1 (5.1)	
PPY5800	2974	2.85	12/35	0.30	2.4	6.5 (4.7)	8.5 (4.9)	
PPYSD115800	3458	1.95	11/24	0.41	3.0	6.9 (5.6)	8.4 (5.8)	10.9
PPY4900	2842	2.77	12/36	0.31	2.3	6.3 (4.6)	8.3 (4.8)	
PPYSD114900	3563	2.54	11/27	0.33	2.8	7.4 (5.8)	9.5 (6.2)	13.1
PPYH114900	3592	2.25	11/27	0.37	2.7	7.5 (6.0)	9.3 (6.4)	12.3

[a]Main pore size maxima obtained from NLDFT analysis. [a]The values in the parenthesis are excess hydrogen uptake.

The surface area and pore volume in Table 4 shows that increasing the severity of activation (beyond the conditions for PPY4800) by performing the activation at KOH/precursor ratio of 5 (sample PPY5800) leads to no change in surface area but the pore volume increases, which is consistent with 'overactivation. On the other hand, the presence of sawdust in the precursor (sample PPYSD115800) enables an increase in surface area to ca. 3500 m^2g^{-1} but with a lowering of the pore volume. In the same manner, increasing the severity of activation by performing the activation at 900 ºC (sample PPY4900) leads to a decrease in surface area and increase in pore volume due to 'overactivation'. Greater surface area (ca. 3600 m^2g^{-1}) may, however, be achieved by adding raw sawdust (sample PPYSD114900) or sawdust hydrochar (sample PPYH114900) to the precursor mix. The achievement of higher surface area has very positive consequences for hydrogen storage as shown in Figure 10, and summarised in Table 4. In all cases the pre-mix precursor samples have much better excess hydrogen uptake (up to 33% higher at 20 and 40 bar) compared to the PPY-only carbons. In general, the pre-mix precursor samples also have higher total hydrogen storage capacity in the pressure range up to 100 bar on account of their better excess hydrogen uptake. The volumetric uptake of the pre-mix samples) is also much higher than that of the equivalent PPY-only samples (Supporting Figure S10) with the excess volumetric uptake of the former being almost twice that of the later. The deliverable hydrogen capacity (100 to 5 bar at 77 K) is also impressive (Table S6).

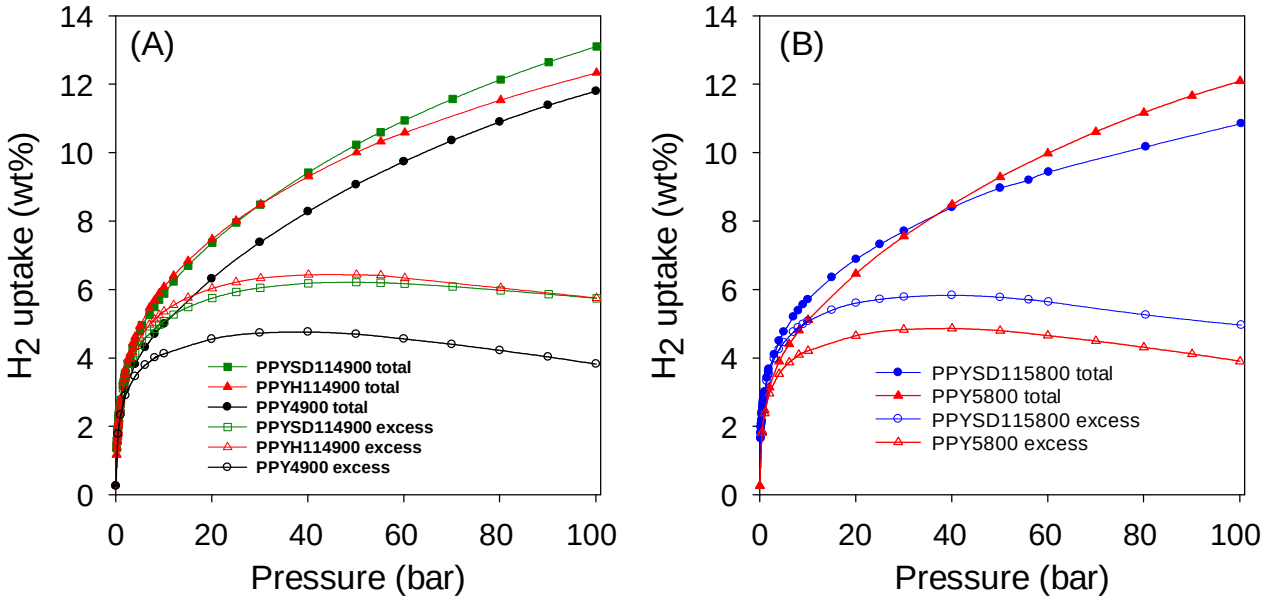

Figure 10. Hydrogen uptake isotherms of activated carbons derived from polypyrrole only (PPY5800 and PPY4900) or pre-mixed precursors containing polypyrrole and raw sawdust (A) or polypyrrole and sawdust-derived hydrochar (B).

4. Conclusions

Homogeneous activated carbons were successfully prepared from pre-mixed precursors containing polypyrrole and sawdust or sawdust-derived hydrochar. The properties of the carbons prepared from pre-mixed precursors were compared to those of carbons generated singly from each of the precursors under similar activation conditions. The pre-mixed precursors offer carbon materials with ultrahigh surface area (up to 3815 m^2 g^{-1}) and pore volume (up to ~2.6 cm^3 g^{-1}) comprising of mainly two pore systems; one pore size system in the micropore range (6 - 12 Å) and the other in the mesopore range (22 – 35 Å). The mix of mesoporosity and microporosity can be tailored by choice of precursor mix to the extent that some samples are predominantly microporous or mesoporous despite there being no change in the activation conditions. This ability to modulate the porosity depending on the precursor mix is related, in part, to the elemental composition of the carbonaceous starting materials, and especially the molar ratio of oxygen to carbon (i.e., O/C molar ratio). It was found that a high O/C ratio favoured ease of activation and

generation of greater mesoporosity. We demonstrate that knowledge of the O/C ratio of carbonaceous matter allows prediction of their activation behaviour, likely porosity and micropore/mesopore mix.[45,93] The level of activation at which increasingly high surface area can be obtained could be extended by use of pre-mixed precursors in a manner not possible for single precursors. Thus it was possible to achieve much higher surface area with the pre-mix precursors than is possible with any one of the precursors when used singly. The N-content of the carbons was found to be dependent on the amount of polypyrrole in the precursor mix. However, the N-content was generally low to very low and did not appear to have any direct influence of the gas uptake properties of the carbons. The pre-mix derived carbons exhibit hydrogen storage capacity that is much higher than can be attained by single-precursor derived samples. The carbons, thus, have excellent excess hydrogen uptake of up to 3.6 wt% and 6.7 wt% (at -196 ºC and 1 or 20 bar, respectively), which translates to total uptake of 8.1 wt% (at -196 ºC and 20 bar). The best performing carbons achieve up to 10.0 wt% total hydrogen storage at 40 bar, which is much higher than that of many currently available benchmark materials. Overall, the hydrogen storage performance of the pre-mix precursor derived carbons is comparable to or outperform many bench mark materials such as MOFs with respect to storage capacity, including gravimetric uptake, volumetric uptake and deliverable hydrogen capacity for pressure swing (100 to 5 bar at 77 K) adsorption conditions.

Supporting Information

Supporting information accompanying this paper, including details of calculation of total hydrogen uptake, and six tables and ten figures is available.

Acknowledgements

We thank the government of the Kingdom of Saudi Arabia for funding a PhD studentship for Norah Balahmar. This work was supported by the Engineering and Physical Sciences Research Council grant [EP/M000567/1] for the Nottingham Gas Adsorption Analysis Suite. RM thanks the Royal Society for a Research Grant, and for a Royal Society Wolfson Research Merit Award.

References

1. L. Schlapbach and A. Züttel, *Nature*, 2001, **414**, 353.
2. U. Eberle, B. Muller and R. von Helmot, *Energy Environ. Sci*., 2012, **5**, 8780.
3. S. Choi, J. H. Drese and C. W. Jones, *ChemSusChem*, 2009, **2**, 796.
4. K. Z. House, A. C. Baclig, M. Ranjan, E. A. van Nierop, J. Wilcox and H. J. Herzog, *Proc. Natl. Acad. Sci. U.S.A.*, 2011, **108**, 20428.
5. M. E. Boot-Handford, J. C. Abanades, E. J. Anthony, M. J. Blunt, S. Brandani, N. Mac Dowell, J. R. Fernandez, M. C. Ferrari, R. Gross, J. P. Hallett, R. S. Haszeldine, P. Heptonstall, A. Lyngfelt, Z. Makuch, E. Mangano, R. T. J. Porter, M. Pourkashanian, G. T. Rochelle, N. Shah, J. G. Yao and P. S. Fennell, *Energy Environ. Sci.*, 2014, **7**, 130.
6. T. C. Drage, C. E. Snape, L. A. Stevens, J. Wood, J. W. Wang, A. I. Cooper, R. Dawson, X. Guo, C. Satterley and R. Irons, *J. Mater. Chem.*, 2012, **22**, 2815.
7. A. Züttel, *Mater. Today*, 2003, **6**, 24.
8. E. Poirier, R. Chahine and T. K. Bose, *Int. J. Hydrogen Energy*, 2001, **26**, 831.
9. M. Sevilla, A. B. Fuertes and R. Mokaya R. *Energy Environ. Sci*., 2011, **3**, 1400.
10. J. Burress, M. Kraus, M. Beckner, R. Cepel, C. Wexler and P. Pfeifer, *Nanotechnology*, 2009, **20**, 204026.
11. Z. Yang, Y. Xia and R. Mokaya, *J. Am. Chem. Soc.*, 2007, **129**, 1673.
12. M. de la Casa-Lillo, F. Lamari-Darkrim, D. Cazorla-Amoros and A. Linares-Solano, *J. Phys. Chem. B*, 2002, **106**, 10930.
13. T. S. Blankenship, N. Balahmar and R. Mokaya, *Nat. Commun.*, DOI: 10.1038/s41467-017-01633-x.
14. E. Masika and R. Mokaya, *Energy Environ. Sci*., 2014, **7**, 427.
15. N. Balahmar, A. M. Lowbridge and R. Mokaya, *J. Mater. Chem. A*, 2016, **4**, 14254.

16. J. P. Marco-Lozar, M. Kunowsky, F. Suarez-Garcia, J. D. Carruthers and A. Linares-Solano, *Energy Environ. Sci.*, 2012, **5**, 9833.
17. M. Sevilla, R. Foulston and R. Mokaya, *Energy Environ. Sci.*, 2010, **3**, 223.
18. C. Robertson and R. Mokaya, *Micropor. Mesopor. Mater.*, 2013, **179**, 151.
19. H. W. Langmi, J. W. Ren, B. North, M. Mathe, D. Bessarabov, *Electrochemica Acta*, 2014, 128, 368.
20. S. Y. Ding and W. Wang, *Chem. Soc. Rev.*, 2013, **42**, 548.
21. L. J. Murray, M. Dincă and J. R. Long, *Chem. Soc. Rev.*, 2009, **38**, 1294.
22. O. K. Farha, A. O. Yazaydın, I. Eryazici, C. D. Malliakas, B. G. Hauser, M. G. Kanatzidis, S. T. Nguyen, R. Q. Snurr and J. T. Hupp, *Nat. Chem.*, 2010, **2**, 944.
23. S. S. Han, H. Furukawa, O. M. Yaghi and W. A. Goddard, *J. Am. Chem. Soc.*, 2008, **130**, 11580.
24. H. Furukawa, N. Ko, Y. B. Go, N. Aratani, S. B. Choi, E. Choi, A. O. Yazaydin, R. Q. Snurr, M. O'Keeffe, J. Kim and O. M. Yaghi, *Science*, 2010, **329**, 424.
25. E. Klontzas, E. Tylianakis and G. E. Froudakis, *Nano Lett.*, 2010, **10**, 452.
26. H. Furukawa and O. M. Yaghi, *J. Am. Chem. Soc*., 2009, **131**, 8875.
27. M. Sevilla, A. B. Fuertes and R. Mokaya, *Int. J. Hydrogen Energy*, 2011, **36**, 15658.
28. L. Wei and G. Yushin, *Nano Energy*, 2012, **1**, 552.
29. B. Adeniran and R. Mokaya, *Nano Energy*, 2015, **16**, 173.
30. J. C. Wang and S. Kaskel, *J. Mater. Chem.*, 2012, **22**, 23710.
31. M. Sevilla and R. Mokaya, *Energy Environ. Sci*., 2014, **7**, 1250.
32. Y. D. Xia, Z. X. Yang and Y. Q. Zhu, *J. Mater. Chem. A*, 2013, **1**, 9365.
33. M. Cox and R. Mokaya, *Sustainable Energy Fuels*, 2017, **1**, 1414.
34. M. Sevilla, R. Mokaya and A. B. Fuertes, *Energy Environ. Sci.*, 2011, **4**, 2930.
35. Y. W. Zhu, S. Murali, M. D. Stoller, K. J. Ganesh, W. W. Cai, P. J. Ferreira, A. Pirkle, R. M. Wallace, K. A. Cychosz, M. Thommes, D. Su, E. A. Stach and R. S. Ruoff, *Science*, 2011, **332**, 1537.
36. M. Sevilla, N. Alam and R. Mokaya, *J. Phys. Chem. C*, 2010, **114**, 11314.
37. M. Sevilla and A. B. Fuertes, *Energy Environ. Sci.*, 2011, **4**, 1765.
38. M. Nandi, K. Okada, A. Dutta, A. Bhaumik, J. Maruyama, D. Derks and H. Uyama, *Chem. Commun.*, 2012, **48**, 10283.
39. N. Balahmar, A. C. Mitchell and R. Mokaya, *Adv. Energy Mater.*, 2015, **5**, 1500867.
40. M. Sevilla, W. Sangchoom, N. Balahmar, A. B. Fuertes and R. Mokaya, *ACS Sustainable. Chem. Eng.*, 2016, **4**, 4710.

41. M. Sevilla, C. Falco, M. M. Titirici and A. B. Fuertes, *Rsc Advances*, 2012, **2**, 12792.
42. H. M. Coromina, D. A. Walsh and R. Mokaya, *J. Mater. Chem.*, 2016, **4**, 280.
43. M. Sevilla, P. Valle-Vigon and A. B. Fuertes, *Adv. Funct. Mater.*, 2011, **21**, 2781.
44. B. Adeniran and R. Mokaya, *Chem. Mater.*, 2016, **28**, 994.
45. X. Zhu, Y. Liu, F. Qian, C. Zhou, S. Zhang and J. Chen, *ACS Sustainable. Chem. Eng.*, 2015, **3**, 833.
46. E. Haffner-Staton, N. Balahmar and R. Mokaya, *J. Mater. Chem. A*, 2016, **4**, 13324.
47. F. C. Wu, R. L. Tseng and R. S. Juang, *Sep. Purif. Technol.*, 2005, **47**, 10.
48. E. A. Hirst, A. Taylor and R. Mokaya, *J. Mater. Chem.* A, 2017, **6**, 12393.
49. N. Balahmar, A. Al-Jumialy and R. Mokaya, *J. Mater. Chem. A*, 2017, **5**, 12330.
50. M. Sevilla and A. B. Fuertes, *Chem. Eur. J.*, 2009, **15**, 4195.
51. H. S. Kambo and A. Dutta, *Energy Conv. Manag.*, 2015, **105**, 746.
52. J. X. Cai, B. Li, C. Y. Chen, J. Wang, M. Zhao and K. Zhang, *Bioresour. Technol.*, 2016, **220**, 305.
53. S. Nizamuddin, N. S. J. Kumar, J. N. Sahu, P. Ganesan, N. M. Mubarak and S. A. Mazari, *Can. J. Chem. Eng.*, 2015, **93**, 1916.
54. W. Sangchoom and R. Mokaya, *ACS Sustainable Chem. Eng.*, 2015, **3**, 1658.
55. M. Sevilla, J. A. Maciá-Agulló and A. B. Fuertes, *Biomass Bioenergy*, 2011, **35**, 3152.
56. J. C. Wang, A. Heerwig, M. R. Lohe, M. Oschatz, L. Borchardt and S. Kaskel, *J. Mater. Chem.*, 2012, **22**, 13911.
57. L. D. Acqua, C. Tonin, R. Peila, F. Ferrero and M. Catellani, *Synthetic Metals*, 2004, **146**, 213.
58. G. Milczarek and O. Inganäs, *Science*, 2006, **312**, 1780.
59. J-S. M. Lee, M. E. Briggs, T. Hasell, and A. I. Cooper, *Adv. Mater.* 2016, **28**, 9804.
60. J. Tabačiarová, M. Mičušík, P. Fedorko and M. Omastová, *Polym. Degrad. Stab*, 2015, **120**, 392.
61. T-M. Wu, H-L. Chang and Y-W. Lin, *Polym. Int.* 2009, **58**, 1065.
62. M. C. Tellez-Juarez, V. Fierro, W. Zhao, N. Fernandez-Huerta, M. T. Izquierdo, E. Reguera and A. Celzard, *Int. J. Hydrogen Energy*, 2014, **39**, 4996.
63. Y. D. Xia, G. S. Walker, D. M. Grant and R. Mokaya, *J. Am. Chem. Soc.*, 2009, **131**, 16493.
64. Y. D. Xia, R. Mokaya, D. M. Grant and G. S. Walker, *Carbon*, 2011, **49**, 844.
65 N. Alam and R. Mokaya, *Energy Environ. Sci.*, 2010, **3**, 1773.
66. Y. Xia and R. Mokaya, *J. Phys. Chem. C*, 2007, **111**, 10035.

67. G. Yushin, R. Dash, J. Jagiello, J. E. Fischer and Y. Gogotsi, *Adv. Funct. Mater.*, 2006, **16**, 2288.
68. B. Panella, M. Hirscher and S. Roth, *Carbon*, 2005, **43**, 2209.
69. H. L. Wang, Q. M. Gao and J. Hu, *J. Am. Chem. Soc.*, 2009, **131**, 7016.
70. T. S. Blankenship and R. Mokaya, *Energy Environ. Sci.*, 2017, **10**, 2552.
71. U. Eberle, B. Müller and R. von Helmolt, *Energy Environ. Sci.*, 2012, **5**, 8780.
72. U. Eberle and R. von Helmolt, *Energy Environ. Sci.*, 2010, **3**, 689.
73. D. A. Gómez-Gualdrón, Y. J. Colón, X. Zhang, T. C. Wang, Y. S. Chen, J. T. Hupp, T. Yildirim, O. K. Farha, J. Zhang and R. Q. Snurr, *Energy Environ. Sci.*, 2016, **9**, 3279.
74. N. Texier-Mandoki, J. Dentzer, T. Piquero, S. Saadallah, P. David and C. Vix-Guterl, *Carbon*, 2004, **42**, 2744.
75. S. K. Bhatia and A. L. Myers, *Langmuir*, 2006, **22**, 1688.
76. I. Cabria, M. J. López and J. A. Alonso, *Carbon*, 2007, **45**, 2649.
77. A. Pacula and R. Mokaya, *J. Phys. Chem. C*, 2008, **112**, 2764.
78. Y. Gogotsi, C. Portet, S. Osswald, J. M. Simmons, T. Yidirim, G. Laudisio and J. E. Fischer, *Int. J. Hydrogen Energy*, 2009, **34**, 6314.
79. Y. Yan, X. Lin, S. Yang, A. J. Blake, A. Dailly, N. R. Champness, P. Hubberstey and M. Schroder, *Chem. Commun*., 2009, 1025.
80. P. García-Holley, B. Schweitzer, T. Islamoglu, Y.Liu, L. Lin, S. Rodriguez, M. H. Weston, J. T. Hupp, D. A. Gómez-Gualdrón, T. Yildirim, and O. K. Farha, *ACS Energy Lett*. 2018, **3**, 748.
81. D. A. Gómez-Gualdrón, T. C. Wang, P. García-Holley, R. M. Sawelewa, E. Argueta, R. Q. Snurr, J. T. Hupp, T. Yildirim and O. K. Farha, *ACS Appl. Mater. Interfaces* 2017, **9**, 33419.
82. A. Ahmed, Y. Liu, J. Purewal, L. D. Tran, A. G. Wong-Foy, M. Veenstra, A. J. Matzger and D. J. Siege, *Energy Environ. Sci*. 2017, **10**, 2459.
83. J. Purewal, D. Liu, A. Sudik, M. Veenstra, J. Yang, S. Maurer, U. Muller and D. J. Siegel, *J. Phys. Chem. C* 2012, **116**, 20199.
84. J. Purewal, D. Liu, J. Yang, A. Sudik, D. Siegel, S. Maurer and U. Mueller, *Int. J. Hydrogen Energy* 2012, **37**, 2723.
85. A. Dailly and E. Poirier, *Energy Environ. Sci*. 2011, **4**, 3527.
86. R. Zacharia, D. Cossement, L. Lafi and R. Chahine, *J. Mater. Chem.* 2010, **20**, 2145.
87. Y. Peng, V. Krungleviciute, I. Eryazici, J. T. Hupp, O. K. Farha and T. Yildirim, *J. Am. Chem. Soc*. 2013, **135**, 11887.

88. Y. Ming, J. Purewal, D. Liu, A. Sudik, C. Xu, J. Yang, M. Veenstra, K. Rhodes, R. Soltis, J. Warner, M. Gaab, U. Müller, D. J. Siegel, *Micropor. Mesopor. Mater*., 2014, **185**, 235.
89. S. E. Bambalaza, H. W. Langmi, R. Mokaya, N. M. Musyoka, J. Ren and L. E. Khotseng, *J. Mater. Chem. A*, 2018, **6**, 23569.
90. D. Alezi, Y. Belmabkhout, M. Suyetin, P. M. Bhatt, Ł. J. Weseliński, V. Solovyeva, K. Adil, I. Spanopoulos, P. N. Trikalitis, A.Emwas and M. Eddaoudi, *J. Am. Chem. Soc*., 2015, **137**, 13308.
91. H. Nishihara, P. X. Li, L. X. Hou, M. Ito, M. Uchiyama, T. Kaburagi, A. Ikura, J. Katamura, T. Kawarada, K. Mizuuchi and T. Kyotani, *J. Phys. Chem. C* 2009, **113**, 3189.
92. N. P. Stadie, J. J. Vajo, R. W. Cumberland, A. A. Wilson, C. C. Ahn, and B. Fultz, *Langmuir* 2012, **28**, 10057.
93. C. Falco, J. Marco-Lozar, D. Salinas-Torres, E. Morallón, D. Cazorla-Amorós, M. Titirici and D. Lozano-Castello, *Carbon*, 2013, **62**, 346.

Graphical Abstract

Carbons derived from pre-mixed precursors (for example polypyrrole and sawdust) have surface area and hydrogen uptake that is not achievable for equivalent single precursor samples; pre-mixing allows hitherto impossible modulation of porosity in a predictable manner.